Nonradiative transport of atomic excitation in Na vapor

Arthur G. Zajonc* and A. V. Phelps†

Joint Institute for Laboratory Astrophysics, University of Colorado and National Bureau of Standards, Boulder, Colorado 80309

(Received 12 December 1980)

Measurements are reported which show the effect of nonradiative losses at a gas-window interface on the backscattered fluorescence intensity for Na vapor at frequencies in the vicinity of the resonance lines near 589 nm. The Na $3P_{1/2,3/2}$ states are excited with a low-intensity single-mode tunable dye laser at high Na densities and the frequency integral of the backscattered fluorescence intensity in the $D1$ and $D2$ lines is measured. As the laser is tuned through resonance, the loss of atomic excitation to the window appears as a sharp decrease in the frequency-integrated fluorescence intensity. For example, at 7×10^{20} atoms m^{-3} the fluorescence intensity decreases by a factor of 4 in a frequency interval of 4 GHz. Measured absolute fluorescence intensities versus laser frequency are compared with predictions made using the theory of Hummer and Kunasz which includes both radiative and nonradiative transport processes. The agreement between theory and experiment is remarkably good when one considers that the theory contains only one unknown coefficient, i.e., the reflection coefficient for excited atoms at the windows. In our case the excited atoms are assumed to be completely destroyed at the window.

I. INTRODUCTION

In this paper we report the results of an experimental study of excited state losses in sodium vapor due to collisions of the excited atoms with a boundary. An early experimental study of resonance fluorescence in Hg vapor by Hansen and Webb[1] has been interpreted by Phelps and Chen[2] as showing that the collisions of excited mercury atoms with the window determine the magnitude of the diffusely emitted fluorescence when the excited atoms are produced close to the window as occurs when the gas density is high and when resonance line excitation is used. Evidence for the deexcitation of excited atoms on collision with the windows has also been obtained from studies of the specular reflection of laser radiation at a glass-sodium vapor interface[3] and from vacuum ultraviolet (vuv) absorption spectra in high-density xenon.[4] Conflicting results as to the importance of excited atom-window collisions have been obtained using the Hanle effect.[5] However, backscattered fluorescence experiments by Heering[6] and by Fujimoto and Phelps[7] using broadband excitation and low resolution measurements of fluorescence showed a relatively small effect caused by nonradiative transport. We show in this paper that using laser excitation allows separation of the effects of radiative and nonradiative transport of resonance radiation in such fluorescence experiments.

The theory of radiative transfer[8-10] normally applied to the transport of resonance excitation neglects excited-atom diffusion, i.e., the motion of the excited atoms is neglected except as it affects the absorption and emission profile through the Doppler effect. Formalisms have recently been developed[2,11-15] which include the diffusion of excited atoms as a means of nonradiative excited-atom transport. These theories predict an excited-atom population density orders of magnitude smaller near a boundary than do the purely radiative treatments. The present experiments test the ability of these theories to predict the absolute intensities of scattered radiation in a situation where losses to a boundary are significant. We make a detailed comparison between experimental results and the solution of the transport equations given by Hummer and Kunasz[12] as formulated in the computer program developed by Kunasz and Kunasz for a three-level system.[13]

Section II contains a summary of the recent theoretical treatments of the combined radiative and nonradiative transport of the excitation associated with the resonance states of atoms. In Sec. III we discuss the experimental apparatus while in Sec. IV we present the results of the experiment. The results are compared with theory in Sec. V.

II. THEORY OF EXPERIMENT

The treatments of the transport of low-intensity resonance radiation by Kenty,[16] by Holstein,[8] and by Biberman[9] showed that, although this problem cannot be solved by ordinary diffusion theory, reasonably simple solutions of the transport equation are possible. In these papers atomic motion entered in only through line shape effects and the absorption and emission profiles were assumed to be identical, i.e., complete redistribution of the radiation was assumed to occur at each absorption event. In treating radiative processes ahead of a shockwave, Biberman and Veklenko[17] presented a transport equation which included the mass flow of excited atoms. McIntyre and Fowler attempted to model the effects of the diffusion of excited atoms and incomplete frequency redistribution in infinite parallel plane geometry.[18] Phelps and McCoubrey[19] and Phelps and Chen[2] extended the

work of Holstein and Biberman to include diffusion of excited atoms by adding a diffusion loss term to the rate equation for the excited atoms. For two-level atoms located between infinite parallel plane boundaries (actually windows) their equation describing the production and loss of excited atoms of density $n(z)$ is

$$F(\omega_L)k(\omega_L)\exp[-k(\omega_L)z/\cos\theta] = An(z) - A\int_0^d n(z')K(|z'-z|)\,dz' - D\frac{d^2n(z)}{dz^2} + C_{21}n(z). \quad (1)$$

According to the left-hand side of Eq. (1), excited-state atoms are created by the laser incident at an angle θ to the normal and of photon flux $F(\omega_L)$. The absorption coefficient at the laser frequency is $k(\omega_L)$. At the low intensities of these experiments $k(\omega_L)$ and the ground-state density N are independent of position. The first term on the right-hand side of Eq. (1) is the rate of loss due to spontaneous decay, where A is the Einstein coefficient for spontaneous radiation and $n(z)$ is the excited-state population density as a function of the depth z, into the cell. The second term on the right-hand side is the Holstein-Biberman term which describes the excited-atom production resulting from the absorption of resonance radition. The kernel $K(|z'-z|)$ is the probability that a photon emitted at z' will be absorbed at z. Thus, the first two terms on the right-hand side of Eq. (1) represent the radiative transport of the energy of the excited atoms.

The next to last term on the of Eq. (1) is the diffusive term in which we are particularly interested. To a good approximation the diffusion coefficient is given by the expression[19]

$$D = \frac{kT}{M\langle\sigma v\rangle N}, \quad (2)$$

where k is the Boltzmann constant, T is the vapor temperature, and M is the atomic mass. Here $\langle\sigma v\rangle$ is the rate coefficient for momentum transfer collisions of the excited atoms with ground-state atoms and is taken to be equal to twice the rate coefficient for excitation transfer collisions[8,19,20] between excited and ground-state atoms. This theory shows that $\langle\sigma v\rangle$ is independent of the gas temperature. The factor of 2 in $\langle\sigma v\rangle$ takes into account the fact that to a good approximation these excitation transfer collisions are equivalent to 180° scattering collisions in the center of mass frame. Because of the large values of $\langle\sigma v\rangle$ for resonance states the diffusion coefficients calculated using this relation are typically several hundred times smaller than the usual gas-kinetic diffusion coefficients such as used by some authors[6,14,18,21] in estimating the importance of this process. The last term in Eq. (1) represents the quenching of the excited atoms, for example by Na_2 molecules, with a rate coefficient C_{21} as measured by Lam *et al.*[22] Collision excitation of resonance atoms is neglected in the two-level model described by Eq. (1). The assumptions, such as complete frequency redistribution and isotropic scattering, made in deriving the radiative terms in Eq. (1) are discussed in detail by Holstein[8] and Biberman.[9] The assumptions are expected to be valid at the high gas densities of the present experiments. The very approximate solutions of Eq. (1) obtained by Phelps and Chen[2] gave very good agreement with experiment[1] and so served to demonstrate the importance of nonradiative transport in Hg vapor.

Lagarkov and Medvedeva[11] derive an equation essentially the same as Eq. (1) but modified to include gas flow and diffusion terms of interest for shockwave experiments. In their first paper analytic solutions for the excited-atom density are found for distances exceeding one effective mean-free path away from the surface bounding the excited volume. Their second paper presents analytic solutions near the boundary which show that for a nonreflecting boundary the excited-atom densities are orders of magnitude lower than those determined by the Holstein-Biberman equation which omits the diffusion term in Eq. (1). Numerical solutions of the equivalent of Eq. (1) have been obtained by Düchs *et al.*[14] for the case of the emission of resonance radiation from a plasma. However, since these authors assume complete reflection of excited atoms at the boundary they find that the effect of adding diffusion is to increase the excited-atom density at the boundary and so to increase the fluorescence at line center. This is just the opposite of the result obtained for a boundary which does not reflect the excited atoms.

The approach used by Hummer and Kunasz[12] is to write separate equations for radiative transport and for the transport of excited atoms. For a two-level atom these equations are

$$\mu\frac{d}{d\tau}I_p(x,\mu,\tau) = \phi(x)\left(I_p(x,\mu,\tau) - \frac{An(\tau)}{B_{12}N}\right) \quad (3)$$

and

$$v_0\,\mu k\frac{d}{d\tau}I_n(\mu,\tau) = (A + C_{21} + N\langle\sigma v\rangle)I_n(\mu,\tau) - \frac{N\langle\sigma v\rangle n(\tau)}{4\pi} - \frac{N(B_{12}\bar{J} + C_{12})}{4\pi}. \quad (4)$$

Here,

$$n(\tau)=2\pi\int_{-1}^{1} I_n(\mu,\tau)\,d\mu \tag{5}$$

is the excited-atom density at an optical depth $\tau = kz$, while I_n is the particle intensity of excited atoms at that depth moving in the direction θ measured relative to the outward normal at the entrance window and $\mu=\cos\theta$. Similarly, the mean radiation intensity $\bar{J}(t)$ is related to the normalized line profile $\phi(x)$ and the photon intensity $I_p(x,\mu,\tau)$ by

$$\bar{J}(\tau)=\tfrac{1}{2}\int_{-1}^{1} d\mu \int_{-\infty}^{\infty} dx\phi(x) I_p(x,\mu,\tau)\,. \tag{6}$$

The line profile $\phi(x)$ used is the Voigt profile, i.e., it includes both Doppler and collision broadening. Here x is the normalized frequency measured from line center. Equation (3) relates the spatial attenuation of the radiative intensity to the difference between the photon absorption by ground-state atoms and the photon production by spontaneous emission of the excited atoms. Stimulated emission can be neglected at the low laser intensities of our experiment. Equation (4) relates the attenuation of the intensity of excited atoms to the loss by radiation and deexcitation, the net scattering by collisions, the production by photon absorption and reradiation, and the production by collisional excitation. In Eqs. (3) and (4), B_{12} is the Einstein coefficient for absorption, $v_0=(2kT/M)^{1/2}$ is the single atomic speed used to characterize the motion of the excited atoms, and C_{12} is the rate coefficient for thermal excitation of the ground-state atoms to the resonance state. These authors also discuss the boundary conditions appropriate to Eqs. (3) and (4) and the method of including the incident radiation. It should be noted[23] that when the angular distributions of the photon and particle intensities can be represented using the first two terms of a spherical harmonic expansion Eqs. (3) and (4) can be reduced to the equivalent Eq. (1). This point brings out one of the advantages of the Hummer and Kunasz solution relative to earlier work, i.e., the more accurate treatment of highly anisotropic angular distributions of radiant and particle intensities, such as found near an absorbing boundary.

Cipolla and Morse[15] have also presented treatments of the coupled radiative and nonraditive transfer problem using kinetic theory. Their treatment differs from that of Hummer and Kunasz in that they solve for the velocity distribution of the atoms. However they consider conditions for which radiative decay occurs sufficiently more frequently than excitation transfer collisions so that they can neglect collisions. The Na densities in the experiment reported in this paper are high enough so that excitation transfer collisions occur more frequently than does spontaneous emission so that the Hummer and Kunasz theory is appropriate for our purposes.

In order to investigate the effects of nonradiative transport we take advantage of the variation of absorption length, $1/k(\omega_L)$, as a function of detuning from the resonance frequency. As can be seen from the left-hand side of Eq. (1), the depth of laser penetration is determined by the exponential term with $k(\omega_L)$ varying with the laser frequency. As we tune away from line center the laser radiation penetrates deeper into the cell creating excited-state sodium atoms far away from the window. One may therefore expect the losses due to collisions with the window will be largest for zero detuning where the radiation is absorbed near the window. Such losses should become increasingly less significant as the laser is tuned further and further from resonance. This effect is responsible for the observation that excited-atom destruction at the window is relatively difficult to detect when "white" light excitation is used.[7]

The theoretical results with which our experimental data are compared were obtained using the extension of Eqs. (3) and (4) reported by Kunasz and Kunasz.[13] Their solution (designated SLAB3) treats a three-level atom, e.g., the $3\,^2P_{3/2}$ and $3\,^2P_{1/2}$ excited states and the $3\,^2S_{1/2}$ ground state of Na. Their program has been further modified by Fujimoto and Phelps[7] to take account of the 1.77 GHz hyperfine splitting (HFS) of the ground state of sodium and by us to include partial redistribution of the incident photon in the first scattering event. The latter modification, which made use of multiple scattering theory,[23] had little effect on the calculated results and will not be considered further. The coefficients used in the comparison with experiment are listed in Table I. Resonance-broadening coefficients are approximately the mean of the experimental values of Niemax and Pichler[24] and the theoretical values of Carrington, Stacey, and Cooper.[25] Excitation transfer rate coefficients were scaled from line broadening data using ratios of these coefficients from Carrington, Stacey, and Cooper.[25] The cross sections for collisional transfer of excitation between the $P_{3/2}$ and $P_{1/2}$ fine structure components were taken from Pitre and Krause.[26] Finally, quenching coefficients for excited Na by Na_2 molecules C_{21} and C_{31} were determined from the experimental work of Lam *et al.*,[22] including approximate allowance for backfeeding from the $a\,^3\Pi$ state and radiative decay of $a\,^3\Pi$ atoms to the $X\,^1\Sigma$ state.

In order to show the general behavior predicted

by the theory, we first show predictions made using the program of Kunasz and Kunasz[13] as modified to include hyperfine structure. The calculated excited-state populations as a function of distance from the window for detuning of 0 and 4 GHz are shown in Fig. 1. In this case the excited atoms are assumed to be de-excited on striking the window. For line center excitation the excited-state population density is found to peak at 3×10^{-6} m from the boundary. This distance is about equal to the optical depth for absorption at line center. On the other hand, for 4-GHz detuning, the peak in the excited-state population density occurs some 20 times deeper into the cell. Clearly, one expects wall losses to be smaller in this latter case.

Figure 2 shows the calculated variation with laser frequency of the integral of the fluorescence signal over the $D2$ resonance line. Unless otherwise noted, the coefficients used in these calculations were those of Table I scaled to a sodium density of 10^{21} atoms m^3. This integrated line fluorescence is plotted as a function of laser detuning from the center of the $D1$ line for a range of diffusion coefficients and boundary conditions. The solid and dashed curves are for 100% absorption and 100% reflection of excited atoms at the window, respectively. Thus, the dashed curve shows the profile expected if destruction of the ex-

TABLE I. Parameters used for comparison with experiment. As in Ref. 13, the levels $3^2S_{1/2}$, $3^2P_{1/2}$, and $3^2P_{3/2}$ are designated by 1, 2, and 3, respectively.

Process	Symbol	Value used	Other values
Temperature	T	702 K	
Na ground-state density	N	6.9(20)[a] m^{-3}	
	A_{21}	6.28(7)[b] sec^{-1}	
	A_{31}	6.30(7)[b] sec^{-1}	
Collisional damping coefficient (FWHM)	$\Delta\omega_2$	4.5(−13) $\frac{\text{rad m}^3}{\text{sec}}$	5.8(−13)[24] 2.95(−13)[25]
	$\Delta\omega_3$	5.4(−13) $\frac{\text{rad m}^3}{\text{sec}}$	6.8(−13)[24] 4.79(−13)[25]
Voigt damping parameter	a_2	2.5(−2)[c]	
	a_3	2.8(−2)[c]	
Excited-atom elastic scattering rate coefficient	$\langle\sigma v\rangle_2$	2.7(−13)[d] m^3/sec	5.9(−13)[e]
	$\langle\sigma v\rangle_3$	3.0(−13)[d] m^3/sec	9.6(−13)[e]
Transfer from $3^2P_{3/2}$ to $3^2P_{1/2}$ and its reverse	C_{32}	1.4(6)[26] sec^{-1}	
	C_{23}	2.7(6)[26] sec^{-1}	
Collisional quenching	C_{31}	7.2(3)[22] sec^{-1}	
	C_{21}	7.2(3)[22] sec^{-1}	
Absorption coefficient at line maximum (with HFS)	k_2(max)	1.835(5)[f] m^{-1}	
	k_3(max)	3.66(5)[f] m^{-1}	
Excited-atom reflection coefficient	R	0.0	

[a] 6.9(20) means 6.9×10^{20}.

[b] W. L. Wiese, M. W. Smith, and B. M. Miles, *Atomic Transition Probabilities* II. *Sodium through Calcium*, National Stand. Ref. Ser., U. S. Nat. Bur. Stand. 22, 1969.

[c] Calculated using coefficients of this table and formulas of Ref. 12.

[d] Calculated by multiplying the coefficients for self-broadening (HWHM) of Niemax and Pichler (Ref. 24) by the respective ratios of the coefficient for the transfer of population to that for relaxation of optical coherence from Carrington, Stacey, and Cooper (Ref. 25). The factor of 2 discussed in connection with Eq. (2) was inadvertently omitted.

[e] These values are twice the rate coefficients for the transfer of population calculated using the theory of Carrington, Stacey, and Cooper (Ref. 25).

[f] Calculated using Voigt profiles and including HFS.

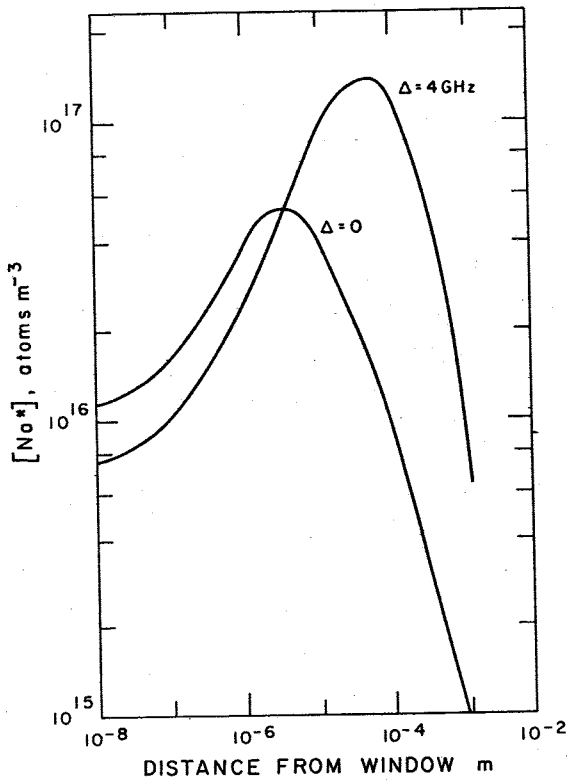

FIG. 1. Theoretical excited-state densities for two laser detunings as a function of distance from window. Conditions are Na density of 7×10^{20} atoms m^{-3}, monochromatic excitation of $P_{3/2}$ state. The plotted population is for the $P_{1/2}$ state and an incident flux of about twice the maximum value used in our experiment, i.e., 10 W/m^2. Hyperfine splitting was included.

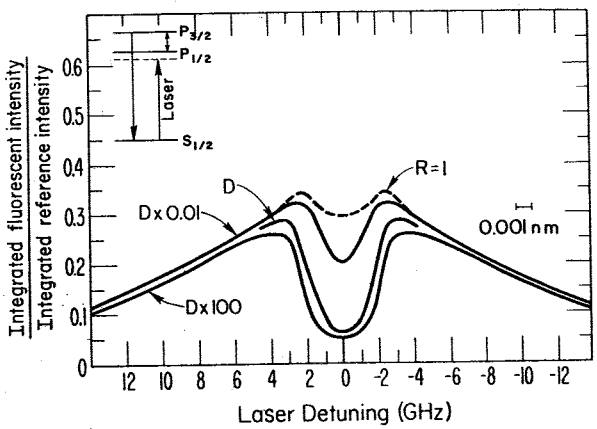

FIG. 2. Theoretical fluorescent intensity profiles. The frequency integrated fluorescence intensity in the Na D2 line emergent in the backward direction relative to that expected for a perfectly diffuse surface is given as a function of laser detuning from the center of the D1 line. The dashed line shows predicted intensitites if wall quenching is negligible (unit excited-atom reflection coefficient). Solid lines show the effect of variation of the momentum transfer rate coefficient on the emergent intensity. The Na density was taken as 1×10^{21} atoms m^{-3}. HFS is not included.

cited atoms at the boundaries is negligible. The dip in the dashed curve at line center is the result of the competition between reradiation and excitation transfer between the $^2P_{1/2}$ and $^2P_{3/2}$ states. In the remainder of this paper we assume that the excited atoms are completely deexcited at the window. The only difference in the coefficients used in the calculations for the three solid curves is the value used for the momentum transfer rate coefficient $\langle \sigma v \rangle$, which affects the diffusion coefficient D through Eq. (2), and the excited-atom transport through the elastic scattering term in Eq. (4). The profile marked D shows the theoretical predicted behavior, namely increasing fluorescence intensity as one approaches line center and a sharp dip at line center due to nonradiative losses. From these curves it is seen that if the momentum-transfer rate coefficient $\langle \sigma v \rangle$ were smaller by a factor of 100 (multiplying D by 100), the integrated intensity curve shows a slightly deeper and wider dip at zero detuning. At line center this case approaches the conditions for which excited atom-ground state collisions are unimportant as considered by Cipolla and Morse.[15] Conversely, if the momentum-transfer rate coefficient is increased by two orders of magnitude, thereby decreasing the mean-free path between collisions and therefore decreasing the importance of nonradiative losses to the window, the curve marked $D \times 0.01$ is the result. As expected in this instance the dip at zero detuning is much shallower than the previous case. The relatively small change in the minimum when the momentum-transfer rate coefficient is reduced by a large factor (D to $D \times 100$) results from the fact that for our conditions the photon absorption length at line center is roughly equal to the mean-free path of the excited atoms, i.e., increasing the excited-atom mean-free path used in the calculations by a factor of 100 does not increase greatly the fraction of the atoms colliding with the window before spontaneous emission. This means that the results presented in this paper are not a sensitive test of the value of $\langle \sigma v \rangle$ used in the calculations.

Figure 3 shows the percent of the incident energy lost via wall quenching as a function of detuning from line center. This calculation was made using the same coefficients as for Fig. 2 and shows that at line center the losses to the window by nonradiative transport are about 65% of the incident energy. Note that the energy lost to the window via the $^2P_{3/2}$ state is much smaller than the loss via the $^2P_{1/2}$ state because of the finite rate of collisional excitation transfer between these states.[26]

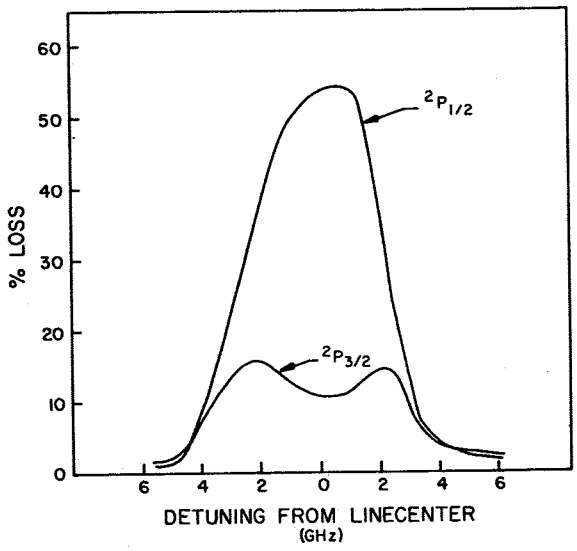

FIG. 3. Nonraditive losses relative to input power calculated from SLAB3 (including HFS) for a Na density of 1×10^{21} atoms m^{-3}. Losses for both the $P_{1/2}$ and $P_{3/2}$ states are shown as a function of laser detuning from line center of the $D1$ ($P_{1/2}\rightarrow S_{1/2}$) transition.

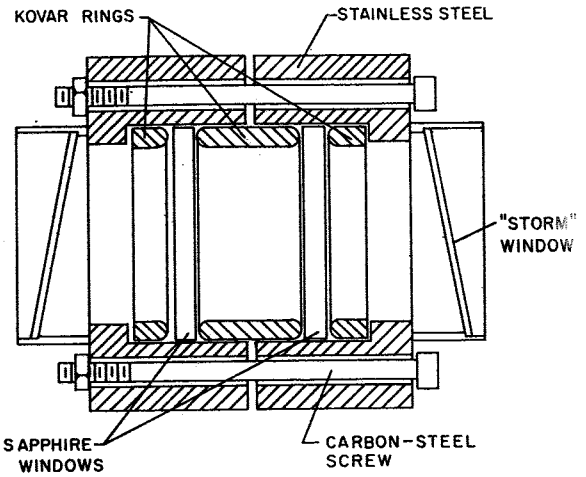

FIG. 5. Cross section of the Na vapor cell. Cu gaskets (not shown) are placed between the inner Kovar ring and the inside of each window. Carbon-steel bolts maintain the compression necessary for sealing. Thin sapphire "storm windows" are placed over the main windows to reduce convective cooling and eliminate Na deposition on the windows (see Ref. 27).

III. EXPERIMENTAL PROCEDURE AND APPARATUS

The schematic diagram of the experimental apparatus is shown in Fig. 4. The sodium cell C shown in Fig. 5 is of a special design which allows operation up to 500 °C. The details of its construction are given elsewhere.[27] The gap between the front and back sapphire windows was 8.6 mm. The cell and sidearm temperatures could be controlled independently by ovens 01 and 02 and were monitored continuously by several thermocouples. The sodium cell was maintained at a temperature somewhat higher than the sidearm assembly and outer windows were added to avoid condensation of sodium on the cell windows. Before vacuum distilling sodium from the high-purity sodium ampule into the sidearm, the entire assembly was evacuated and baked. A pressure of $\sim3\times10^{-6}$ Pa was obtained.

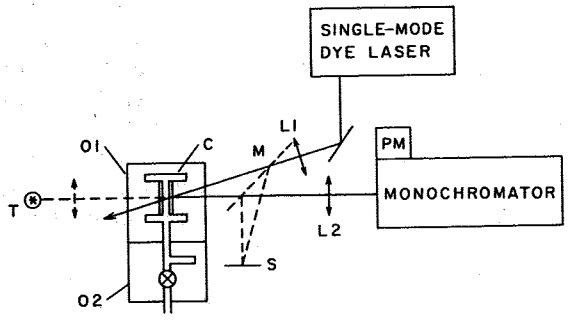

FIG. 4. Block diagram of the experiment. The output beam of the single-mode dye laser is expanded by L1 and directed on the entrance window of the sodium cell C. Fluorescent radiation is focused onto the monochromator lens L2. Oven O1 is the cell oven and O2 is the sidearm and reservoir oven.

The source of monochromatic radiation was an argon-ion pumped, cw dye laser operated single mode and tuned electronically with an intracavity etalon. The spectral line width of the output laser beam was approximately 200 MHz at a power level of 30 mW. The mode structure of the dye laser was continuously monitored by a scanning Fabry-Perot interferometer. Mode hops occurred once every two to four minutes. The laser beam passed through a neutral density filter of unit optical density, a beam-expanding telescope L1, an iris diaphragm, and a beam splitter before passing into the sodium cell at an angle of 15° to the window normal. The input intensity was continuously monitored by a semiconductor photodiode and was always less than 5 W/m^2. The fluorescent signal was found to be a linear function of incident intensity[28] between 0.5 and 5 W/m^2. The fluorescence signal emitted normal to the window was focused on the 24 μm entrance of a 1-m Czerny-Turner monochromator with $f/8.7$, a dispersion of 0.83 nm/mm and a limiting spectral resolution of 10^{-2} nm or 9 GHz. The exit slit of the monochromator was opened to approximately 300 μm when integrating the fluorescence intensity over either the $D1$ or $D2$ line. The photon flux from the monochromator was measured by a photon counting chain consisting of a multialkali photomultiplier operated at dry ice temperature, a pre-

amplifier, an amplifier-discriminator, and a scalar. Count rates were typically 20 000 counts per second with integration times of 1 sec. Both the laser and the monochromator could be scanned under the control of a mincomputer which also normalized the signal count rate to the laser intensity. The monochromator scan was provided by a stepping motor with 0.01 nm per step increments, whereas the dye-laser scan was performed by the intracavity etalon in 560-MHz steps. The raw data along with the laser input intensities were stored on magnetic tape for later analysis.

Sodium densitities were calculated from the data of Nesmeyanov.[29] As a check, absorption measurements were made using a white light source T (tungsten-filament-iodine lamp) operated at a color temperature of about 2900 K. The measured equivalent widths and line broadening data[24] for the $D1$ and $D2$ lines could then be used to calculate the sodium densities. These two density determinations were within 15% of that calculated from the vapor pressure curve.

The normalization of the radiant intensity scattered by the Na cell to the incident radiative flux was made by placing a mirror M of known reflectivity into the laser beam such that the reflected laser beam was incident on a white surface S in the same geometry as that of the cell.[7] The white surface was $BaSO_4$ paint and its scattering efficiency was calibrated using $BaSO_4$ powder[30] stated by the manufacturer to be 99% efficient at the wavelengths of interest when prepared according to instructions. Transmission coefficients of the evacuated quartz-cell windows of the oven, as well as the sapphire input window, were measured and used in the normalization of the data. By this method we were able to determine the ratio of the fluorescent intensity to the intensity of radiation scattered by a perfectly diffuse surface.

IV. RESULTS

Figure 6 shows experimental spectral line profiles obtained for three values of laser detuning from the $D1$ resonance line at 589.6 nm. In each case the monochromator was scanned from 588.6 to 590.0 nm for a fixed laser detuning. The Na density was 3×10^{21} atoms m^{-3}. As can be seen, with excitation at line center the detected linewidth is essentially determined by the monochromator resolution of 0.02 nm. The middle trace shows that if the laser excitation is detuned approximately 4 GHz into the red wing of the $D1$ line, the fluorescence line profiles become broader and the $D2$ line intensity increases while that of the $D1$ line decreases. The broader line profile results from the fact that radiation absorbed deep in the vapor

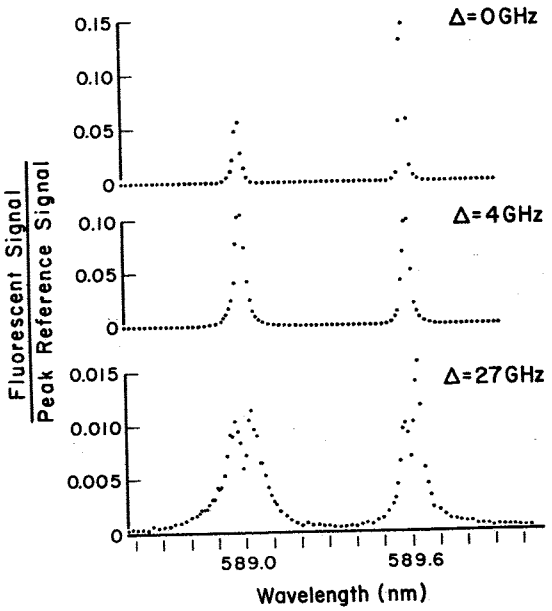

FIG. 6. Normalized fluorescent signal profiles for three values of laser detuning Δ from line center excitation of $P_{1/2}$. The Na density was 3×10^{21} m^{-3}. In the lower trace the peak on the long-wavelength side of the $D1$ line is due to laser light scattered by imperfections in the cell windows. The scattered light signal from the reference white surface has the same frequency dependence as the profiles in the top trace but has unit amplitude.

must be emitted in the wings of the resonance line in order to reach the window.[8,9] The deeper penetration of the laser light also increases the mean lifetime of the excited atoms allowing for greater collisional transfer of excitation to the $P_{3/2}$ component. Finally, for a detuning of 27 GHz, or approximately 0.03 nm, the backscattered line profiles become very broad and display self-absorption at line center. These profiles demonstrate that the $D1$ and $D2$ lines are well separated and that a 300 μm exit slit setting is sufficient to include essentially all of the scattered intensity in either the $D1$ or the $D2$ line.

Scans of the measured fluorescent intensity integrated over the $D1$ and $D2$ lines as a function the laser frequency are shown by the points in Figs. 7 and 8. Experimental runs were made at a variety of densities but detailed theoretical comparisons were made only for Na density of 6.9×10^{20} atoms m^{-3} and cell temperature of 705 K. In these runs stray laser light was measured to be less than 0.6% of the maximum signal.

The theoretical results are shown in Figs. 7 and 8 by the solid lines. The data for $P_{3/2}$ excitation in Fig. 7 clearly show a dip near zero detuning which reflects the expected increase in wall losses. As one would expect, the wall losses for

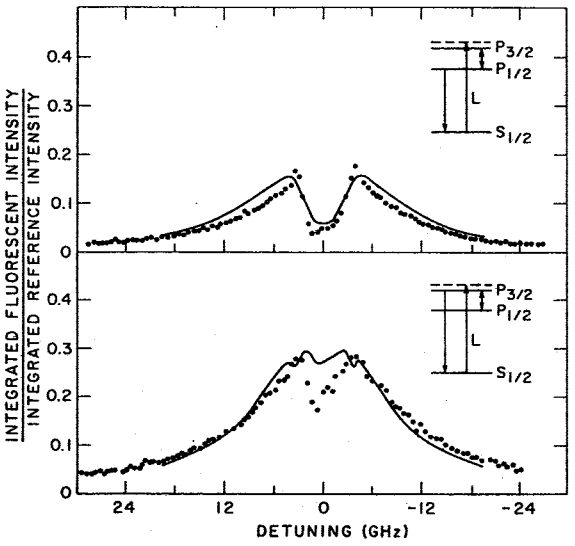

FIG. 7. Top: Integrated fluorescence intensity from $P_{1/2}$ as a function of detuning from $P_{3/2}$ line center. Bottom: Fluorescence from $P_{3/2}$ level with $P_{3/2}$ excitation. The Na density was 6.9×10^{20} m^{-3}. The solid curve shows model predictions. Dots are the measured ratios of the cell fluorescence to the signal scattered by the white surface after correction for window transmission, etc. The experimental data are shifted in frequency for best fit to the theory.

$P_{1/2}$ excitation in Fig. 8 appear smaller due to its smaller absorption coefficient. It is also interesting to note the drastic reduction in sensitized fluorescence, i.e., radiation following energy transfer from the initial excited fine structure component to the second component, when the atoms are excited at resonance. This reflects both the increases loss of excited atoms by radiation and the large wall losses which prevail for these conditions. Calculations such as those plotted in Fig. 3 show that the latter effect is dominant. The asymmetry and structure which consistently appear near line center excitation are attributed to the 1.77-GHz hyperfine splitting of the ground state.

The agreement between theory and experiment is significantly better for $P_{3/2}$ excitation than for $P_{1/2}$ excitation. In the former case the agreement is excellent in all regions except near zero detuning for the $P_{3/2}$-$P_{3/2}$ curve (Fig. 7, top). It is, of course, just this region which is most sensitive to boundary effects. Both here and for the $P_{1/2}$-$P_{1/2}$ (Fig. 8, bottom) results, theory overestimates the experimental results by at least 25%. Inclusion of frequency-coherent scattering of the incident radiation at the first scattering event into the model produced a negligible change in the calculated results at this density. One also notes that since our model assumes complete destruction of the excited atoms at the window it is not possible to lower the calculated intensities at line center by changing the reflection coefficient for the excited atoms at the window.

V. SUMMARY

An experiment has been performed which shows the effect on fluorescent intensity of nonradiative excitation transport to a boundary. In particular, losses due to quenching of excited atoms can be an important and even dominant loss mechanism for certain density and excitation conditions. Funding limitations prevented the more extended analysis of these data necessary to clarify the remaining discrepancies between theory and experiment. Future experiments and analysis should consider the effect of this nonradiative loss of excited atoms on the time dependent decay of the excited atoms and on the propagation of intense laser beams in the region near the boundary.

ACKNOWLEDGMENTS

We wish to thank Chela and Paul Kunasz for their untiring patience and assistance with the further development and use of SLAB3 and J. L. Hall for advice and assistance in connection with the dye laser. We also wish to thank T. Fujimoto and R. Smick for their contributions through the construction of apparatus and the development of computer programs during earlier projects. This research was supported in part by the Advanced Research Projects Agency and was monitored by the Office of Naval Research under Contract No. N00014-76-C-0123 with the University of Colorado.

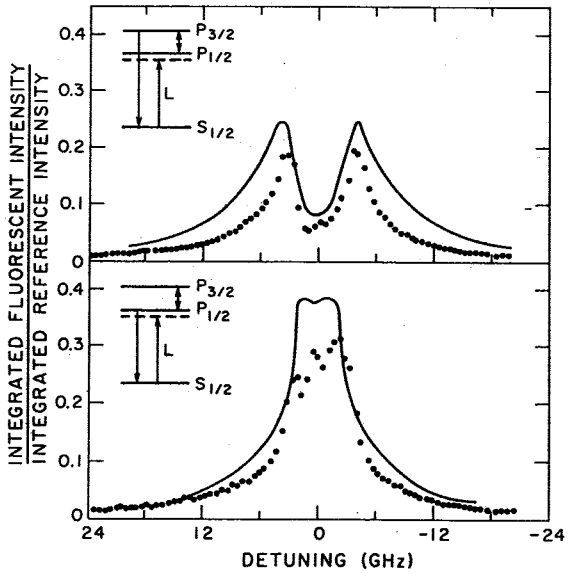

FIG. 8. Same as Fig. 7 but laser excitation of $P_{1/2}$ and detection of $P_{3/2}$ fluorescence (top) and $P_{1/2}$ fluorescence (bottom).

*Present address: Physics Department, Amherst College, Amherst, Massachusetts 01002.
†Staff member, Quantum Physics Division, National Bureau of Standards and Lecturer, Department of Physics, University of Colorado, Boulder, Colorado.

[1]J. M. Hansen and H. W. Webb, Phys. Rev. 72, 332 (1947).

[2]A. V. Phelps and C. L. Chen, Bull. Am. Phys. Soc. 15, 428 (1970). Details are given in the Yearly Summary Technical Reports for Contract No. NR-4725(00), Westinghouse Research Laboratories, June 1969 and September 1970 (unpublished). The approximate theory of these references shows that the effective diffusion coefficient for sodium atoms in the 3P state increases as $N^{1/3}$ for N above about 3×10^{24} m^{-3}. This additional transport is estimated assuming stationary atoms and considering only excitation transfer to nearest-neighbor atoms, i.e., transport by "hopping" of the excitation. Presumably exciton behavior becomes important at the higher Na densities.

[3]M. F. H. Schuurmans, J. Phys. (Paris) 37, 469 (1976); A. L. J. Burgmans and J. P. Woerdman, *ibid.* 37, 677 (1976); A. L. J. Burgmans, M. F. H. Schuurmans, and B. Bölger, Phys. Rev. A 16, 2002 (1977).

[4]T. D. Bonifield, F. H. K. Rambow, G. K. Walters, M. V. McCusker, D. C. Lorents, and R. A. Gutcheck, J. Chem. Phys. 72, 2914 (1980).

[5]B. M. Dodsworth, J. C. Gay and A. Omont, J. Phys. (Paris) 33, 65 (1972); A. L. J. Burgmans, Phys. Rev. A 19, 1954 (1979).

[6]W. Heering, Z. Physik A 274, 91 (1975).

[7]T. Fujimoto and A. V. Phelps, Bull. Am. Phys. Soc. 21, 173 (1976).

[8]T. Holstein, Phys. Rev. 72, 1212 (1947); 83, 1159 (1951).

[9]L. Biberman, Zh. Eksp. Teor. Fiz. 17, 416 (1947); Dokl. Akad. Nauk. SSSR 59, 659 (1948).

[10]D. G. Hummer, J. Quant. Spectrosc. Radiat. Transfer 8,193 (1968); D. G. Hummer and G. B. Rybicki, Annu. Rev. Astron. Astrophys. 9, 237 (1971); V. V. Ivanov, *Transfer of Radiation in Spectral Lines*, translation edited by D. G. Hummer, National Bureau of Standards Special Publication No. 385 (U. S. G. P. O., Washington, D. C., 1973).

[11]A. N. Lagarkov and N. A. Medvedeva, J. Quant. Spectrosc. Radiat. Transfer 13, 209; 13, 225 (1973); 17, 735 (1977).

[12]D. G. Hummer and P. B. Kunasz, J. Quant. Spectrosc. Radiat. Transfer 16, 77 (1976).

[13]C. V. Kunasz and P. B. Kunasz, Comput. Phys. Commun. 10, 304 (1975).

[14]D. F. Düchs and J. Oxenius, Z. Naturforsch. 32a, 156 (1977); D. F. Düchs, S. Rehker, and J. Oxenius, Z. Naturforsch. 33a, 124 (1978).

[15]J. W. Cipolla, Jr. and T. F. Morse, J. Quant. Spectrosc. Radiat. Transfer 22, 365 (1979).

[16]K. Kenty, Phys. Rev. 42, 823 (1932).

[17]L. M. Biberman and B. Veklenko, Zh. Eksp. Teor. Fiz. 37, 164 (1959) [Sov. Phys.—JETP 37, 117 (1960)].

[18]R. G. McIntyre and R. G. Fowler, Astrophys. J. 133, 1055 (1961); R. G. McIntyre and E. M. D'Arcy, J. Appl. Phys. 43, 2251 (1972).

[19]A. V. Phelps and A. O. McCoubrey, Phys. Rev. 118, 1561 (1960).

[20]W. Fursow and A. Vlassow, Phys. Z. Sowjetunion 10, 378 (1936). The factor of 2 used to convert excitation transfer rate coefficients to momentum transfer rate coefficients also occurs in symmetric charge transfer theory. See, for example, A. Dalgarno and M. R. C. McDowell, Proc. Phys. Soc. London 69, 615 (1956).

[21]R. G. Fowler, in *Handbuch der Physik*, edited by S. Flügge (Springer, Berlin, 1956), p. 226.

[22]L. K. Lam, T. Fugimoto, A. C. Gallagher, and M. M. Hessel, J. Chem. Phys. 68, 3553 (1978).

[23]P. J. Chantry, A. V. Phelps, and G. J. Schulz, Phys. Rev. 152, 81 (1966).

[24]K. Niemax and G. Pichler, J. Phys. B 8, 179 (1975).

[25]C. G. Carrington, D. N. Stacey, and J. Cooper, J. Phys. B 6, 417 (1973).

[26]J. Pitre and L. Krause, Can. J. Phys. 46, 125 (1968).

[27]A. G. Zajonc, Rev. Sci. Instrum. 51, 1682 (1980).

[28]This linear behavior, i.e., the absence of saturation effects, is in agreement with predictions of the theory as illustrated by the small degree of fractional excitation calculated for the conditions of Fig. 1. Our attempts to experimentally observe the effects of window losses on the threshold for nonlinear propagation of the laser as a function of frequency were unsuccessful.

[29]An. N. Nesmeyanov, *Vapour Pressure of the Elements*, translated by J. I. Carasso (Academic, New York, 1963).

[30]V. E. Kartachevskaya, H. Korte, and A. R. Robertson, Appl. Opt. 14, 2694 (1975).